Infiltrative Hepatocellular Carcinoma: What Radiologists Need to Know[1]

Arich R. Reynolds, MD
Alessandro Furlan, MD
David T. Fetzer, MD[2]
Eizaburo Sasatomi, MD, PhD
Amir A. Borhani, MD
Matthew T. Heller, MD
Mitchell E. Tublin, MD

Abbreviations: AFP = α-fetoprotein, HCC = hepatocellular carcinoma, LI-RADS = Liver Imaging Reporting and Data System, OPTN = Organ Procurement and Transplantation Network, UNOS = United Network for Organ Sharing

RadioGraphics 2015; 35:371–386

Published online 10.1148/rg.352140114

Content Codes: CT GI MR OI

[1]From the Departments of Radiology (A.R.R., A.F., D.T.F., A.A.B., M.T.H., M.E.T.) and Pathology (E.S.), University of Pittsburgh, 200 Lothrop St, Pittsburgh, PA 15213. Presented as an education exhibit at the 2013 RSNA Annual Meeting. Received March 24, 2014; revision requested July 9 and received August 5; accepted September 4. For this journal-based SA-CME activity, the authors, editor, and reviewers have disclosed no relevant relationships. Address correspondence to A.F. (e-mail: *furlana@upmc.edu*).

[2]**Current address:** Department of Radiology, University of Texas Southwestern Medical Center, Dallas, TX.

SA-CME LEARNING OBJECTIVES

After completing this journal-based SA-CME activity, participants will be able to:

- Discuss the presentation and pathologic features of infiltrative HCC, as well as the prognosis and current therapeutic options for patients with the disease.
- Describe the findings at US, CT, and MR imaging that may facilitate diagnosis of infiltrative HCC.
- Identify the liver diseases that can mimic infiltrative HCC and the imaging findings that are helpful for discriminating the differential diagnoses.

See www.rsna.org/education/search/RG.

Hepatocellular carcinoma (HCC) is one of the leading causes of cancer-related death worldwide. The macroscopic growth pattern of HCC is subdivided into three categories: nodular, massive, and infiltrative. Infiltrative HCC accounts for 7%–20% of HCC cases and is confirmed at pathologic analysis on the basis of the spread of minute tumor nodules throughout large regions of the liver. Infiltrative HCC may represent a diagnostic challenge because it is often difficult to distinguish from background changes in cirrhosis at imaging. Infiltrative HCC usually spreads over multiple hepatic segments, occupying an entire hepatic lobe or the entire liver, and it is frequently associated with portal vein tumor thrombosis. The tumor is usually ill defined at ultrasonography and shows minimal and inconsistent arterial enhancement and heterogeneous washout at contrast material–enhanced computed tomography and magnetic resonance (MR) imaging. The tumor may be more visible among the surrounding liver parenchyma at diffusion-, T1-, and T2-weighted MR imaging. Several liver diseases can mimic the infiltrative appearance of this malignancy, including focal confluent fibrosis, hepatic fat deposition, hepatic microabscesses, intrahepatic cholangiocarcinoma, and diffuse metastatic disease (pseudocirrhosis). The prognosis for patients with infiltrative HCC is poor because the tumor is often markedly advanced and associated with vascular invasion at presentation. Survival after surgical resection is decreased; thus, infiltrative HCC is a contraindication for resection and transplantation. Knowledge of the key tumor characteristics and imaging findings will help radiologists formulate a correct and timely diagnosis to improve patient management.

Introduction

Worldwide, hepatocellular carcinoma (HCC) is the second- and sixth-leading cause of cancer-related death among men and women, respectively (1). HCC arises almost exclusively in the context of underlying cirrhosis, and its incidence is increasing in many developed nations likely because of the increasing prevalence of hepatitis C virus infection and the worsening obesity epidemic (1–4). Recent data reveal that the age-adjusted prevalence of HCC in

TEACHING POINTS

- Although the macroscopic growth pattern of infiltrative HCC is uncommon, none of the histologic features other than its growth pattern is unique to this type of HCC. Despite its name, infiltrative HCC does not have irregular or indistinct margins around each tumor nodule; instead, the tumor nodules of infiltrative HCC are distinct with well-defined borders.
- Portal vein tumor thrombosis is a common finding in patients with infiltrative HCC, often affecting both extra- and intrahepatic branches, with a frequency ranging from 68% to 100%.
- At contrast-enhanced CT and MR imaging, infiltrative HCC may be difficult to discern from underlying heterogeneous cirrhosis because of its permeative appearance, its minimal and inconsistent arterial enhancement, and the heterogeneous washout appearance that occurs during the venous phase.
- The relatively reduced conspicuity of infiltrative HCC on images obtained during the dynamic phases of enhancement likely relates to the permeative infiltrating nature of the tumor and frequent presence of portal vein thrombosis, which results in perfusion changes that can effectively conceal the tumor. Therefore, the tumor may be more visible among the surrounding liver parenchyma on diffusion-, T1-, and T2-weighted MR images than on dynamic contrast-enhanced images.
- Survival after surgical resection is decreased; thus, infiltrative HCC is a contraindication for resection and transplantation.

North America is 6.8 and 2.2 cases per 100,000 persons among men and women, respectively (5). In 50%–60% of these cases, the underlying cause is hepatitis C virus infection; 20% of cases are caused by chronic hepatitis B virus infection; and alcohol consumption, nonalcoholic steatohepatitis, and other causes account for the remaining 20% (5).

With regard to its pathologic characteristics, the macroscopic growth pattern of HCC is subdivided into three categories: nodular, massive, and infiltrative (6). Infiltrative HCC is characterized by the spread of minute tumor nodules throughout a hepatic lobe or the entire liver. Infiltrative HCC has been described as diffuse HCC, cirrhotomimetic-type HCC, or cirrhosis-like HCC (7,8). It has an aggressive course and is associated with a substantially worse prognosis, compared with the nodular HCC subtype (9,10). Infiltrative HCC accounts for approximately 7%–20% of HCC cases (9,11–15) and is reported to be commonly associated with hepatitis B virus infection, particularly in Asia (9,16). Patients with infiltrative HCC may have markedly elevated α-fetoprotein (AFP) values (>10,000 ng/mL) (10,13,17). However, AFP serum level measurement has poor accuracy for diagnosis of HCC (12), and patients with infiltrative HCC may have normal (<20 ng/mL) or only mildly elevated (<400 ng/mL) levels (10,12,13).

Although the imaging appearance of nodular and massive forms of HCC is well defined and routinely described throughout the medical literature, there is a relative paucity of clinical and imaging literature on the infiltrative subtype. Infiltrative HCC frequently represents a diagnostic challenge for radiologists because its ill-defined appearance often makes it difficult to distinguish from changes in underlying cirrhosis. Use of imaging to facilitate the diagnosis of infiltrative HCC is further complicated by a number of diseases with an infiltrative appearance similar to that of the malignancy.

A diagnosis of infiltrative HCC has important implications for patient treatment. Because of decreased survival after surgical resection, patients are usually given local-regional or systemic therapies. Therefore, knowledge of the key tumor characteristics and imaging findings is important for radiologists to formulate a correct and timely diagnosis to improve patient management. This article aims to discuss the pathologic features and imaging appearance of infiltrative HCC, describe the diseases that most commonly have similar findings, and address the prognosis and current treatment options for patients with infiltrative HCC.

Imaging Modalities for Diagnosis of HCC

Imaging plays a crucial role in diagnosis, staging, and treatment of HCC as detailed by multiple practice guidelines (18–21). The most widely used and recommended imaging modalities are ultrasonography (US) and multiphasic contrast material–enhanced computed tomography (CT) and magnetic resonance (MR) imaging. Hepatic US is widely accessible and inexpensive and does not require the use of ionizing radiation. Practice guidelines of the American Association for the Study of Liver Disease and the European Association for the Study of the Liver recommend that abdominal US be performed every 6 months for surveillance in patients at high risk for HCC (18,19). However, image quality is highly operator dependent, varies with transducer and platform, and is affected by the body habitus of the patient. The imaging appearance of HCC at US is nonspecific, and lesions larger than 1 cm in diameter require further evaluation with CT or MR imaging (19). The reported accuracy of US for detection of HCC in the cirrhotic liver is limited and varies substantially. Yu et al (22) described 225 patients with HCC confirmed by pathologic analysis at liver explantation and found that the lesion-based sensitivity of US was only 46%. In this same series, contrast-enhanced CT and MR imaging had per-lesion sensitivities of 65% and 72%, respectively (22). In a meta-analysis by Colli et al (23), the pooled sensitivity of US, CT, and MR imaging

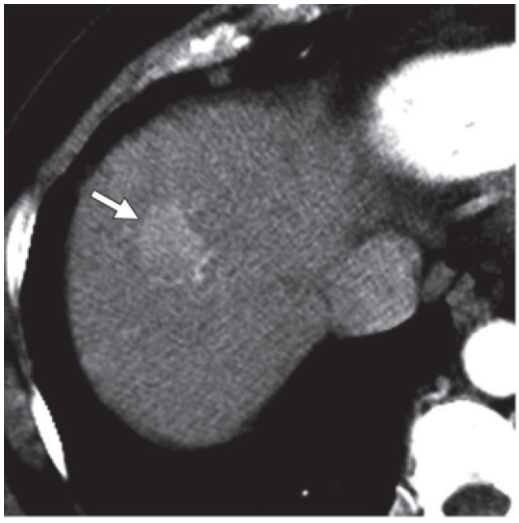

a.

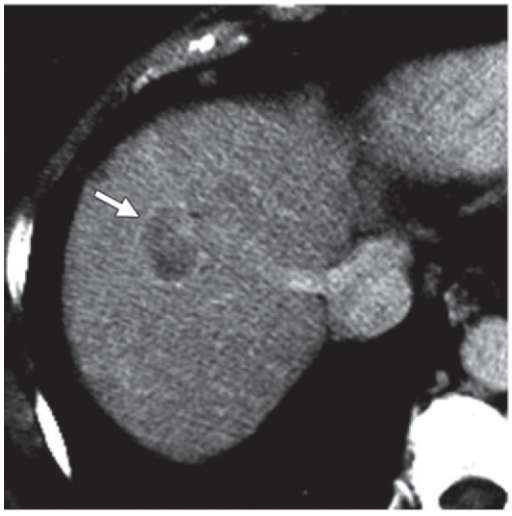

b.

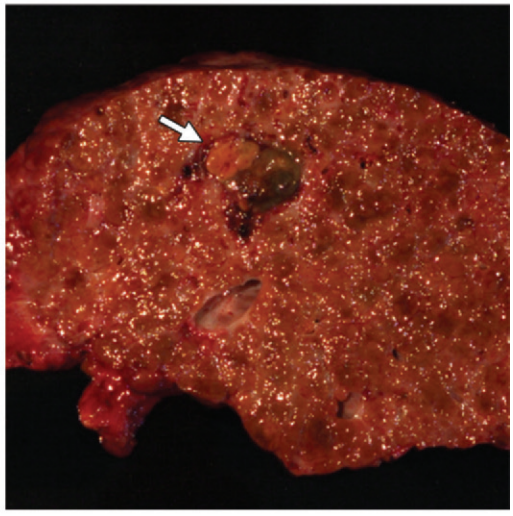

c.

Figure 1. Nodular HCC in a 60-year-old woman with a history of cirrhosis due to nonalcoholic steatohepatitis. **(a)** Axial arterial phase CT image shows a 2.3-cm hypervascular mass (arrow) in the liver dome. **(b)** Axial portal venous phase CT image shows a washout appearance and a capsule (arrow), features that are considered to be diagnostic for HCC. The patient underwent liver transplantation. **(c)** Photograph of the explanted liver shows a well-circumscribed nodule (arrow) with focal hemorrhage, findings that are compatible with HCC. Note the diffusely nodular background parenchyma mixed with fibrotic tissue.

for facilitating the diagnosis of HCC was 48%, 68%, and 81%, respectively.

The diagnosis of HCC can be made at contrast-enhanced multiphasic CT and MR imaging, following fulfillment of highly specific criteria outlined by the policy of the Organ Procurement and Transplantation Network (OPTN) and United Network for Organ Sharing (UNOS) (20). When these criteria are met, the patient may qualify for additional points on the transplantation list without the need for pathologic proof of tumor. OPTN/UNOS policy and the evolving Liver Imaging Reporting and Data System (LI-RADS) have compatible major imaging criteria for the diagnosis of HCC (20,21). Typically, HCC enhances more than the surrounding liver parenchyma during the arterial phase, while it is hypoenhancing relative to the surrounding liver during the portal venous and/or delayed phase (ie, washout appearance) (24,25) (Fig 1). The presence of both a capsule on the delayed phase images and tumor growth are included as major diagnostic criteria in OPTN/UNOS and LI-RADS recommendations (20,21).

According to the most recent OPTN/UNOS policy, CT and MR imaging techniques must meet minimal requirements to facilitate the definitive diagnosis of HCC (20). Multiphasic contrast-enhanced CT should be performed on a multidetector CT scanner (minimum of eight rows) with intravenous injection of weight-based iodinated contrast medium (1.5 mL per kilogram body weight; minimum iodine concentration, 300 mg/mL) at a rate of 4–6 mL/sec. Contrast-enhanced images (minimum of 5-mm reconstruction section thickness) are acquired during the late arterial phase (ie, artery fully enhanced and initial contrast enhancement of the portal vein, approximately 15–20 sec after aortic threshold-based scanning initiation), portal venous phase (approximately 30–60 sec after scan initiation), and delayed phase (>120 sec after contrast material injection).

The recommended minimal technical parameters for dynamic contrast-enhanced MR imaging of the liver are a 1.5-T imagin unit equipped with a phased-array coil. The protocol should include unenhanced gradient-echo T1-weighted dual-echo images and T2-weighted spin-echo images (with and without fat saturation). The core of the protocol is the dynamic study, usually conducted with gradient-spoiled sequences performed before and after intravenous injection of gadolinium-based contrast agent (25). The recommended contrast medium is a weight-based extracellular gadolinium chelate injected intravenously at a rate of 2–3 mL/sec. Contrast-enhanced images should be obtained during the late arterial phase (bolus tracking), the portal venous phase (35–55 sec after arterial phase initiation), and the delayed phase (120–180 sec after contrast material injection) (20,21,26). Many health care centers currently use a gadolinium chelate with combined extracellular or interstitial and hepatobiliary properties for liver imaging, such as gadobenate dimeglumine (MultiHance, Bracco Imaging, Milan, Italy) and gadoxetic acid (Eovist, Bayer-Schering Pharma, Berlin, Germany) (27,28). Contrast material is internalized by normally functioning hepatocytes, and images from the delayed hepatobiliary phase can be obtained after the dynamic study. Although not recognized as a major diagnostic criterion in OPTN/UNOS policy or LI-RADS guidelines, the appearance of a hepatic lesion in a cirrhotic liver (appearing as a focus of nonaccumulation) at MR imaging during the hepatobiliary phase can be suggestive of HCC (27,28). Finally, diffusion-weighted imaging is commonly included in many MR imaging protocols for the liver (29,30).

Pathologic Characteristics of Infiltrative HCC

HCC has been traditionally categorized into three major types based on the Eggel growth pattern classification: nodular, massive, and diffuse (6). The nodular type consists of a single tumor or multiple nodular tumors with clear demarcation. The massive type consists of a large tumor with an unclear boundary that occupies most or all of a hepatic lobe. The infiltrative, or diffuse, type is characterized by the spread of minute tumor nodules throughout an entire lobe or the entire liver without a dominant nodule (Fig 2). Virtually all livers harboring infiltrative HCC have underlying cirrhosis. Infiltrative HCC is often cryptic and can masquerade as cirrhotic nodules; therefore, several authors have referred to infiltrative HCC as cirrhotomimetic-type HCC or diffuse cirrhosis-like HCC (7,8). Many investigators believe that infiltrative HCC frequently, if not always, represents innumerable intrahepatic metastases based on observations that tumor thrombi are frequently present in large perihilar portal veins (31). However, in a recent study of 10 native liver specimens obtained at hepatectomy, no tumor was found in the major branches of either the hepatic or the portal veins, although small-vessel invasion frequently was observed (8). Of note, large-vessel invasion is not necessarily a salient feature of infiltrative HCC.

Although the macroscopic growth pattern of infiltrative HCC is uncommon, none of the histologic features other than its growth pattern are unique to this type of HCC. Despite its name, infiltrative HCC does not have irregular or indistinct margins around each tumor nodule; instead, the tumor nodules of infiltrative HCC are distinct with well-defined borders (Fig 2). Whereas Okuda et al (31) reported diffuse-type cases of HCC that were poorly differentiated, Jakate et al (8) described 10 cases of diffuse HCC that were mostly moderately or well differentiated. Jakate et al (8) also described a general uniformity of grade among multiple nodules in each patient.

Whether infiltrative HCC corresponds to intrahepatic metastases from a single primary tumor or to multiple independent tumors remains controversial. Whereas Okuda et al (31) suggest that infiltrative HCC frequently, if not always, represents intrahepatic widespread portal metastases that occur during a short period, Jakate et al (8) posit that the likelihood of infiltrative HCC being multiclonal is greater because of the lack of a dominant massive nodule.

Imaging of Infiltrative HCC

The spread of minute tumor nodules throughout the liver is the typical pathologic macroscopic appearance of infiltrative HCC. This pattern translates as a permeative ill-defined appearance at US, CT, and MR imaging. Infiltrative HCC usually spreads over multiple hepatic segments, occupying an entire lobe or the entire liver (10,13,17). Moreover, multiple smaller satellite lesions are reported in up to 52% of cases (10,32).

Portal vein tumor thrombosis is a common finding in patients with infiltrative HCC, often affecting both extra- and intrahepatic branches (10,13,17,32–34), with a frequency ranging from 68% to 100%. Moreover, because of the permeative appearance and subtle enhancement of the tumor, portal vein thrombosis may appear as the primary imaging feature (33). Hepatic venous thrombosis is reported less frequently (17). The uses, pitfalls, and limitations of US, CT, and MR imaging for facilitating the diagnosis of infiltrative HCC are described below and summarized in Table 1.

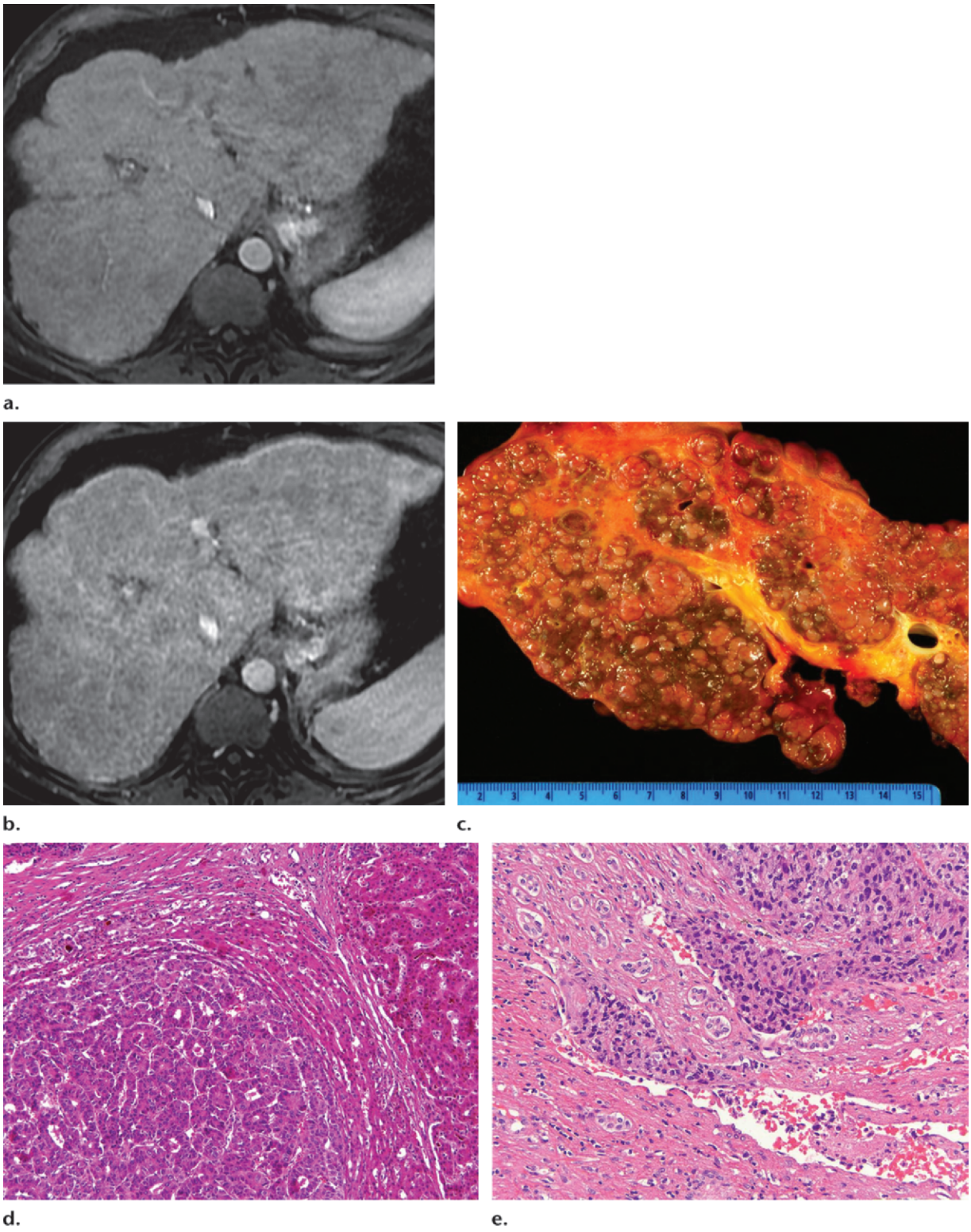

Figure 2. Infiltrative HCC in a 64-year-old man with a history of alcoholic cirrhosis and an elevated serum AFP level (880 ng/mL). **(a)** Contrast-enhanced arterial phase T1-weighted MR image shows no hypervascular lesion. **(b)** Axial portal venous phase T1-weighted MR image shows a reticular appearance of the liver with no discrete lesion visible. The patient did not have tumor thrombosis. **(c)** Cut surface specimen of the explanted liver shows separate and coalescing pink-tan tumor nodules that are approximately the size of cirrhotic nodules. (Scale is in centimeters.) **(d)** Medium-power photomicrograph (original magnification, ×100; hematoxylin-eosin stain) shows expansive growth of the tumor nodules with border-compressing adjacent benign hepatocytes. The tumor shows both a trabecular and a pseudoglandular pattern of growth. **(e)** Medium-power photomicrograph (original magnification ×200; hematoxylin-eosin stain) with higher magnification shows vascular invasion in small vessels in the fibrous septa. All nodules are moderately differentiated, and all lesions are similar in histologic appearance.

Table 1: Advantages and Pitfalls of Various Modalities for Imaging of Infiltrative HCC

Imaging Modality	Advantages	Pitfalls and Limitations
US		
Gray scale	Guidance for biopsy	Tumor and underlying cirrhosis often difficult to distinguish
Color and spectral Doppler	Detection of portal vein thrombosis	Tumor and underlying cirrhosis often difficult to distinguish
Contrast-enhanced CT		
Multiphasic acquisitions after contrast enhancement	Detection helped by presence of washout appearance in the tumor; identification of enhancing tumoral thrombus	Pattern often indistinguishable from fibrosis and nodularity seen in cirrhosis; minimal heterogeneous contrast enhancement during arterial phase
MR imaging		
T2 weighted and diffusion weighted	Increased visibility compared with dynamic study	Nonspecific appearance
Dynamic study after gadolinium chelate injection	Detection helped by presence of washout appearance in the tumor	Minimal heterogeneous contrast enhancement during arterial phase
Hepatobiliary phase (after injection of hepatospecific gadolinium-based contrast material)	Detection and assessment of tumor burden helped by hypointensity	Nonspecific appearance

Ultrasonography

At US, infiltrative HCC appears as an ill-defined area of markedly heterogeneous echotexture and thus is often indistinguishable from cirrhosis (8) (Fig 3). In the study by Yu et al (22), six (50%) of 12 cases of infiltrative HCC that were confirmed with pathologic analysis were not detected at US. Color Doppler US allows real-time evaluation of the hepatic vasculature. At US, malignant portal vein thrombosis is suspected on the basis of the absence of normal blood flow and the presence of a hypoechoic thrombus expanding the vessel (Fig 4). The presence of pulsatile flow in a portal vein thrombus at spectral Doppler examination, although highly specific (95%), is only a moderately sensitive (62%) sign of malignant portal vein thrombosis (35). Contrast-enhanced US may be helpful in differentiating benign and malignant vein thrombi in patients with HCC (36).

US can be used to guide liver biopsy to obtain specimens for testing to confirm HCC. Despite the limitation of US in depicting infiltrative HCC in the context of underlying cirrhosis, anatomic landmarks seen at CT or MR imaging can be used to direct biopsy to the area of concern. US-guided biopsy can also be used to evaluate portal vein thrombus; this procedure has been shown to be effective and well tolerated (37,38) (Fig 5).

Contrast-enhanced CT and MR Imaging

At contrast-enhanced CT and MR imaging, infiltrative HCC may be difficult to discern from underlying heterogeneous cirrhosis because of its permeative appearance, its minimal and inconsistent arterial enhancement, and the heterogeneous washout appearance that occurs during the venous phase (13,33,39,40). The enhancement pattern of infiltrative HCC seen on images obtained during the hepatic arterial phase has been reported as minimal, patchy, or miliary (10,13,17,32,39) (Figs 2, 3, 5, 6). Although arterial hyperenhancement is a key diagnostic feature of nodular and massive HCC, infiltrative HCC may commonly appear as iso- or hypointense on images obtained during the arterial phase (33,34). Washout appearance is a specific CT and MR imaging feature of typical nodular HCC. Hypointensity relative to the surrounding liver parenchyma during the venous phase of enhancement remains a valid sign for the detection of infiltrative HCC (34). However, washout appearance of the tumor is usually reported as irregular and heterogeneous (Figs 2, 3, 5, 6) and is less frequently seen in infiltrative HCC than in other HCC subtypes (13,17,32,40). In a series by Kneuertz et al (10), washout appearance was present in 77.4% of multifocal HCC cases and in only 50.8% of infiltrative HCC cases. Moreover, a reticular appearance of the tumor has been seen on images obtained during the venous and equilibrium phases (10,33,34,39), possibly related to fibrosis (33) (Fig 3). Finally, the tumor generally appears as hypointense on MR images acquired during the hepatobiliary

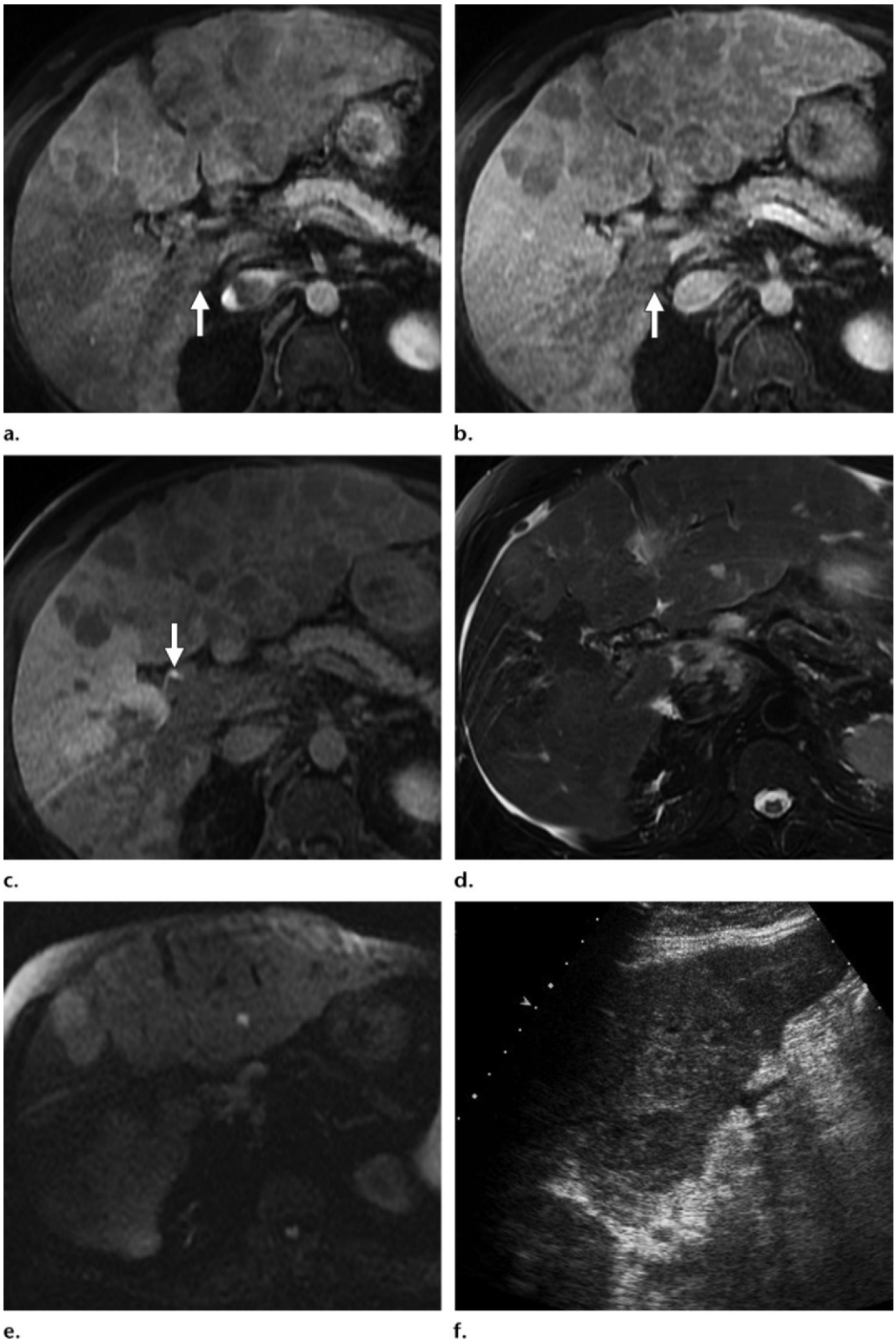

Figure 3. Infiltrative HCC in a 67-year-old man with a history of excessive alcohol use and portal venous thrombosis found at CT performed for follow-up of aortic aneurysm. The patient had a markedly elevated serum AFP level (6880 ng/mL). MR imaging was performed before and after intravenous injection of gadoxetic acid. **(a)** Axial arterial phase T1-weighted MR image shows patchy areas of heterogeneous enhancement diffusely involving the left lobe and posterior segment of the right lobe and extending to the right portal vein (arrow). **(b)** Axial portal venous phase T1-weighted MR image shows heterogeneous washout appearance, with improved delineation of portal venous tumoral thrombosis (arrow). **(c)** Axial hepatobiliary phase T1-weighted MR image obtained 20 minutes after contrast material injection shows hypointensity of the involved areas; note the biliary excretion of contrast material (arrow). **(d, e)** Axial T2-weighted **(d)** and diffusion-weighted (b = 500 sec/mm^2) **(e)** MR images show mild hyperintensity in the involved areas. **(f)** Transverse US image obtained before MR imaging shows findings of cirrhosis, including heterogeneous echotexture and nodular margins without a focal lesion.

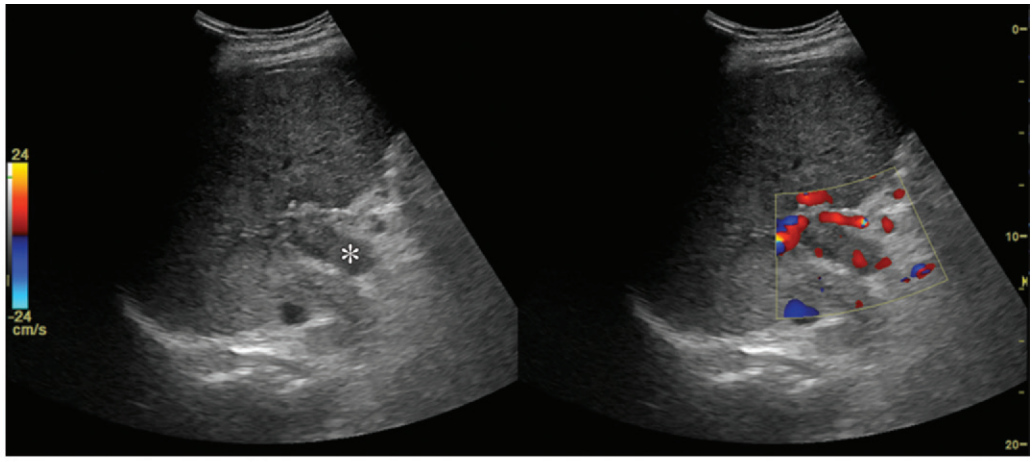

a.

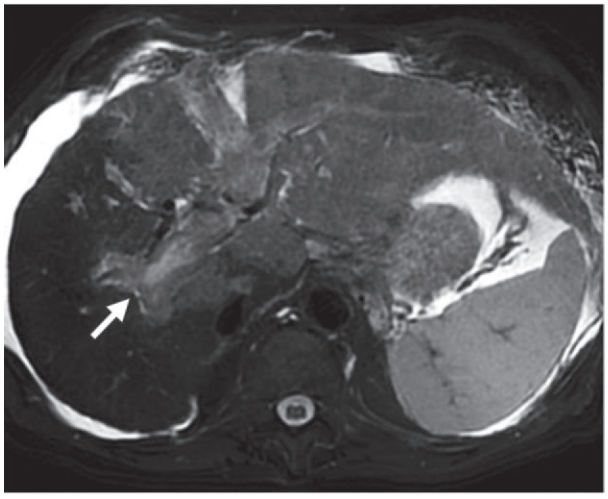

b.

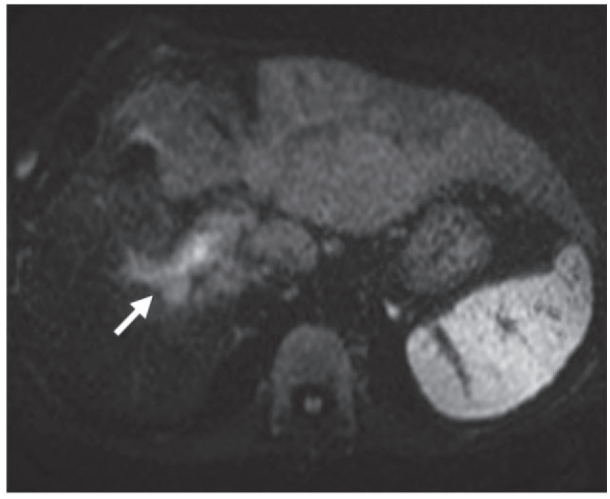

c.

Figure 4. Portal venous tumor thrombosis in a 75-year-old man with a history of alcoholic cirrhosis whose serum AFP level was 50 ng/mL. **(a)** Composite gray-scale (left) and duplex (right) US image shows an expanded and echogenic main portal vein (*), compatible with portal vein thrombosis. Color Doppler evaluation confirmed lack of flow in the vessel. **(b, c)** Axial T2-weighted **(b)** and diffusion-weighted (b = 500 sec/mm^2) **(c)** MR images show large areas of moderately increased signal intensity in the left hepatic lobe. Note the hyperintensity of the right portal vein tumor thrombus (arrow). Percutaneous US-guided biopsy of the lateral segment was performed, and results of examination of the sample were consistent with poorly differentiated HCC.

phase after injection of hepatospecific contrast agent (Fig 3) because of the lack of contrast agent uptake (32,33).

The relatively reduced conspicuity of infiltrative HCC on images obtained during the dynamic phases of enhancement likely relates to the permeative infiltrating nature of the tumor and frequent presence of portal vein thrombosis, which results in perfusion changes that can effectively conceal the tumor (33). Therefore, the tumor may be more visible among the surrounding liver parenchyma on diffusion-, T1-, and T2-weighted MR images than on dynamic contrast-enhanced images (33,34). Infiltrative HCC usually appears to be moderately and heterogeneously hyperintense on T2-weighted images (Figs 3, 4) and homogeneously or heterogeneously hypointense on T1-weighted images (10,13,17,32–34,39). Infiltrative HCC generally appears to be hyperintense, compared with surrounding liver parenchyma, on diffusion-weighted images acquired with high b values (b = 500–800 sec/mm^2) (32–34) (Figs 3, 4).

At contrast-enhanced CT and MR imaging, malignant thrombosis expands the portal vein and shows an enhancement pattern similar to that of the adjacent tumor (41–43) (Figs 3–6). Arterialization of the thrombus has been reported in 8.1% of patients with infiltrative HCC (10). Restricted diffusion (33,43) and increased signal intensity on T2-weighted images (10) have also been described in the context of malignant portal vein thrombosis (Fig 4).

Other Associated Imaging Findings

Intrahepatic biliary ductal dilatation is not a typical feature of infiltrative HCC, although it is reported in 13%–26% of cases (13,32,39). In

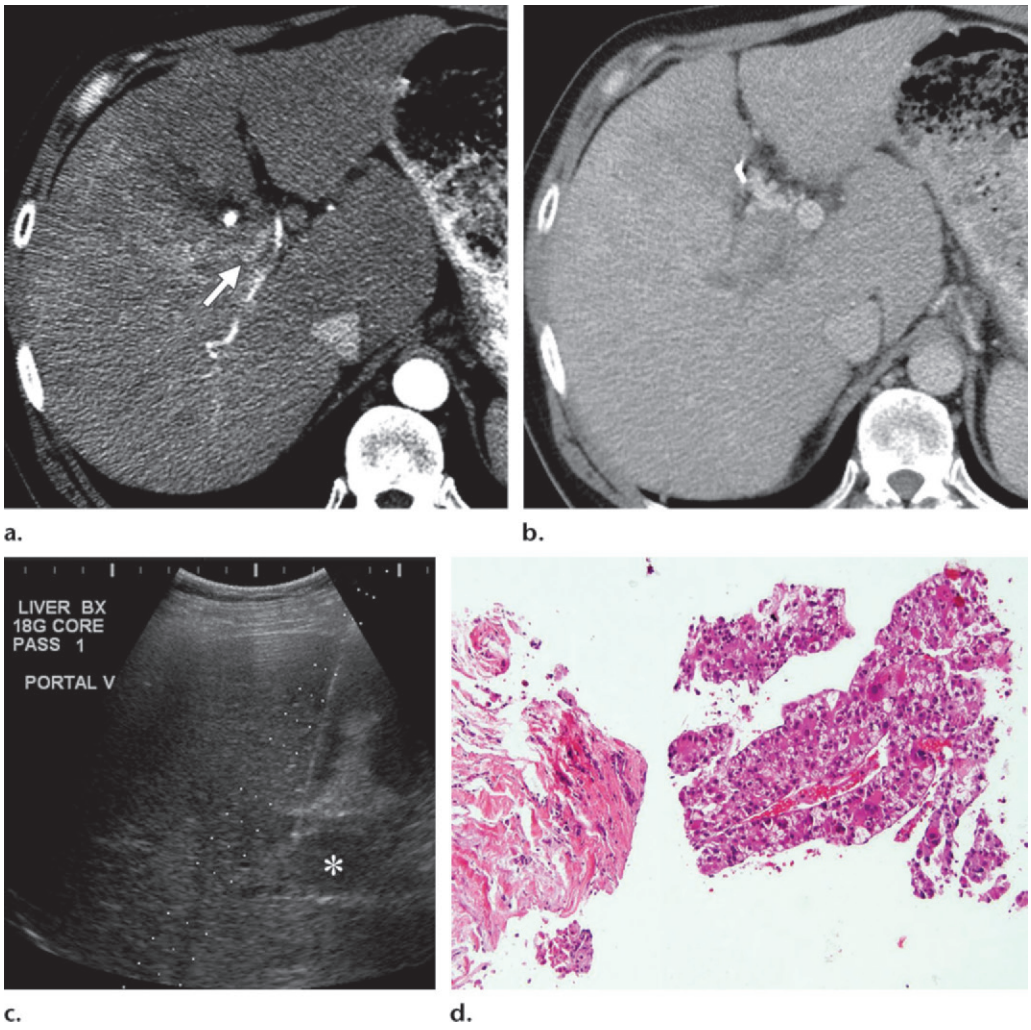

Figure 5. Infiltrative HCC and portal venous tumor thrombosis in a 51-year-old man who presented for surveillance with a history of hepatitis C virus cirrhosis; his serum AFP level was 48 ng/mL. **(a)** Axial arterial phase CT image shows heterogeneous enhancement in segments V and VIII with enhancing thrombosis in the right portal vein (arrow). **(b)** Axial portal venous phase CT image shows vague washout appearance in segments V and VIII. Portal vein tumor thrombosis is better delineated during this phase of imaging. The patient underwent random biopsy of segment V; no evidence of malignancy was found. The patient subsequently underwent US-guided biopsy of the portal vein tumor thrombosis. **(c)** US image shows the thrombosis (*). **(d)** Medium-power photomicrograph (original magnification, ×100; hematoxylin-eosin stain) of the specimen shows moderately differentiated HCC.

10%–22% of cases, the extrahepatic spread of disease affects the upper abdominal lymph nodes (10,13,32,34). Distant metastases have been reported in the lungs, bones, and adrenal glands in 13%–23% of cases (10,13,34).

Mimics of Infiltrative HCC

Multiple diseases affecting the liver, including focal confluent fibrosis, fat deposition, microabscesses, cholangiocarcinoma, and diffuse metastatic disease, can have an imaging appearance similar to that of infiltrative HCC (Table 2).

Focal Confluent Fibrosis

Differentiation of focal confluent fibrosis from malignant invasion may be difficult to determine at CT and MR imaging because replacement of normal hepatocytes, whether by scar or tumor, can alter the hepatic architecture and enhancement pattern. Confluent fibrosis often affects the anterior and medial hepatic segments, is typically peripheral and wedge shaped, and radiates from the porta hepatis (44–46). Unlike infiltrative HCC, confluent fibrosis may result in overlying capsular retraction and vessel crowding (Fig 7) (44–46). At nonenhanced CT, confluent fibrosis typically manifests as areas of low attenuation relative to normal liver; areas of fibrosis are hypointense at T1-weighted MR imaging and mildly hyperintense at T2-weighted MR imaging (Fig 7) (44,45).

Because malignancy may have a similar appearance on T1- and T2-weighted images, analysis of enhancement characteristics is

a.

b.

c.

Figure 6. Infiltrative HCC and portal and hepatic venous tumor thrombosis in a 60-year-old man with a history of hemochromatosis who had a markedly elevated serum AFP level (14,546 ng/mL). **(a)** Axial arterial phase CT image shows minimal heterogeneous enhancement of the right lobe and hypervascular malignant thrombus (arrow) in the right portal vein. **(b)** Axial portal venous phase CT image shows heterogeneous washout appearance in the right hepatic lobe and in the malignant tumor thrombus expanding the right portal vein. **(c)** Catheter angiogram of the proper hepatic artery (obtained for local-regional chemoembolization) shows vascularity of the portal venous tumor thrombus (circle) and hepatic venous thrombus (oval).

critical. Unlike HCC, focal confluent fibrosis generally appears to be hypovascular at early contrast-enhanced imaging and shows delayed enhancement (32,44–46) (Fig 7). Park et al (32) reported that delayed enhancement was seen in seven of eight cases of focal confluent fibrosis and in zero of 19 cases of infiltrative HCC. When a hepatospecific contrast agent is used at MR imaging of the liver, the hepatobiliary phase alone cannot be used for the differentiation of infiltrative HCC and focal confluent fibrosis because both fibrosis and tumor generally lack the ability to uptake contrast agent (Fig 7). In the same study by Park et al (32), images from 18 of 19 cases of infiltrative HCC and five of seven cases of focal confluent fibrosis showed hypointensity during the hepatobiliary phase because of the lack of contrast agent uptake (32). Moreover, the authors showed that the mean apparent diffusion coefficient (± standard deviation) was lower for infiltrative HCC than for focal confluent fibrosis (0.97 cm^2/sec ± 0.19 vs 1.35 cm^2/sec ± 0.39; $P = .001$) and that the frequency of portal vein thrombosis and satellite nodules was higher in patients with infiltrative HCC than in patients with focal confluent fibrosis (32).

Hepatic Fat Deposition

Hepatic fat deposition may occur in a variety of patterns in the liver. The common locations for focal fat or focal fat sparing, such as adjacent to the gallbladder fossa or falciform ligament, may obviate additional evaluation. However, geographic or multifocal nodular patterns of steatosis may mimic infiltrative HCC. Affected areas may appear hypointense on fat-saturated MR images acquired during the hepatobiliary phase after injection of gadolinium chelate with hepatospecific properties (eg, gadobenate dimeglumine and gadoxetic acid) (47,48). Uniform signal loss between dual-echo in-phase and

Table 2: Imaging Features and Distinctions between Infiltrative HCC and Its Mimics

Mimics	Imaging Features	Distinction from Infiltrative HCC
Focal confluent fibrosis	Geographic regions of relatively low attenuation at CT, relative hypointensity on T1-weighted images and mild hyperintensity on T2-weighted images at MR imaging	Often affects the anterior and medial hepatic segments, wedge shaped and radiates from the porta hepatis, capsular retraction, delayed contrast enhancement
Hepatic fat deposition	Geographic and nodular pattern of altered attenuation/signal intensity, affected regions may appear as hypointense at hepatobiliary phase MR imaging	Often distinguishable location (adjacent to gallbladder fossa or falciform ligament), signal loss between dual-echo in-phase and opposed-phase gradient-echo T1-weighted MR images
Hepatic microabscesses	Multiple hypoattenuating lesions at CT, hyperintensity on T2-weighted images with faint restricted diffusion and peripheral or septal contrast enhancement at MR imaging	Clinical history
Intrahepatic cholangiocarcinoma	Ill-defined mass, hypointense on T1-weighted images and hyperintense on T2-weighted images	Irregular peripheral enhancement with gradual centripetal enhancement, capsular retraction, tumor thrombus atypical
Diffuse metastatic disease (pseudocirrhosis)	Diffuse metastatic disease with associated alteration of hepatic morphologic features similar to those of cirrhosis	Clinical history of primary malignancy (eg, breast cancer)

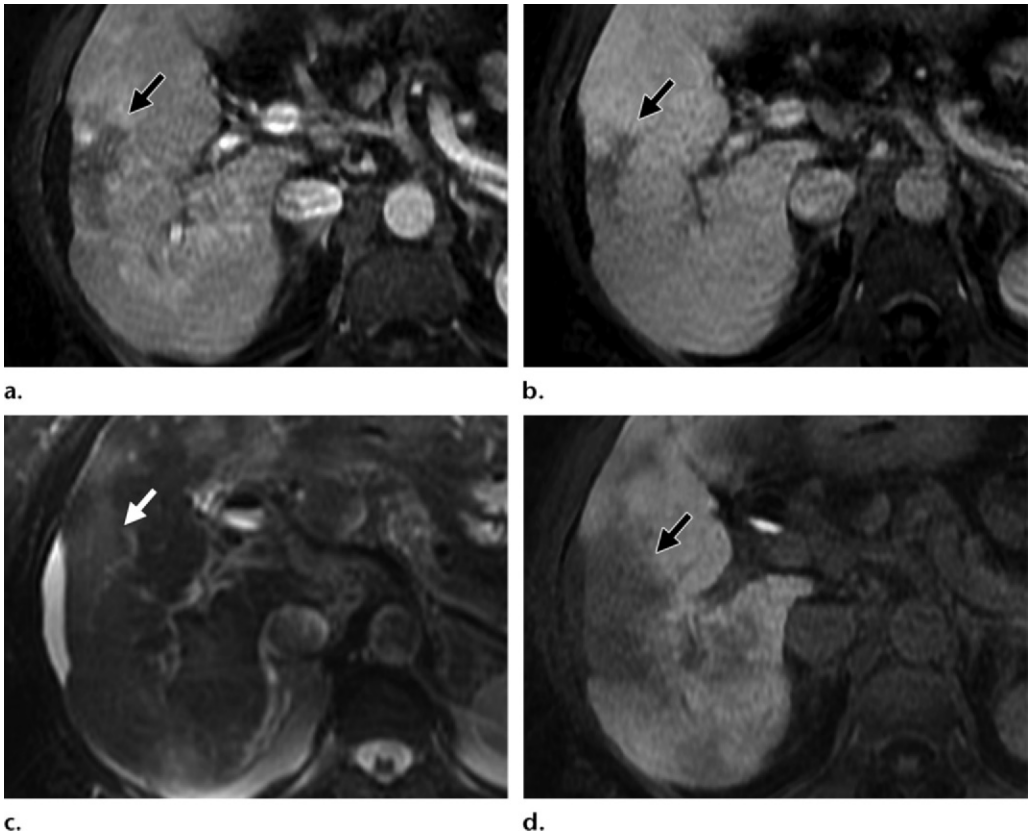

Figure 7. Focal confluent fibrosis in a 63-year-old woman with a history of ulcerative colitis and secondary biliary cirrhosis; she had normal serum AFP and cancer antigen 19-9 levels. The patient was referred for further evaluation of a hepatic mass in segment V that was detected at CT (not shown). **(a, b)** Axial contrast-enhanced T1-weighted MR images obtained during the arterial **(a)** and portal venous **(b)** phases show a large area of signal intensity alteration in segment V (arrow) with early peripheral enhancement and delayed central enhancement. **(c)** Axial T2-weighted MR image shows mild hyperintensity (arrow) in this region. **(d)** Axial hepatobiliary phase T1-weighted MR image obtained 20 minutes after administration of gadoxetic acid shows hypointensity (arrow). Note the associated capsular retraction. US-guided biopsy specimen of this area showed cirrhotic changes without evidence of malignancy.

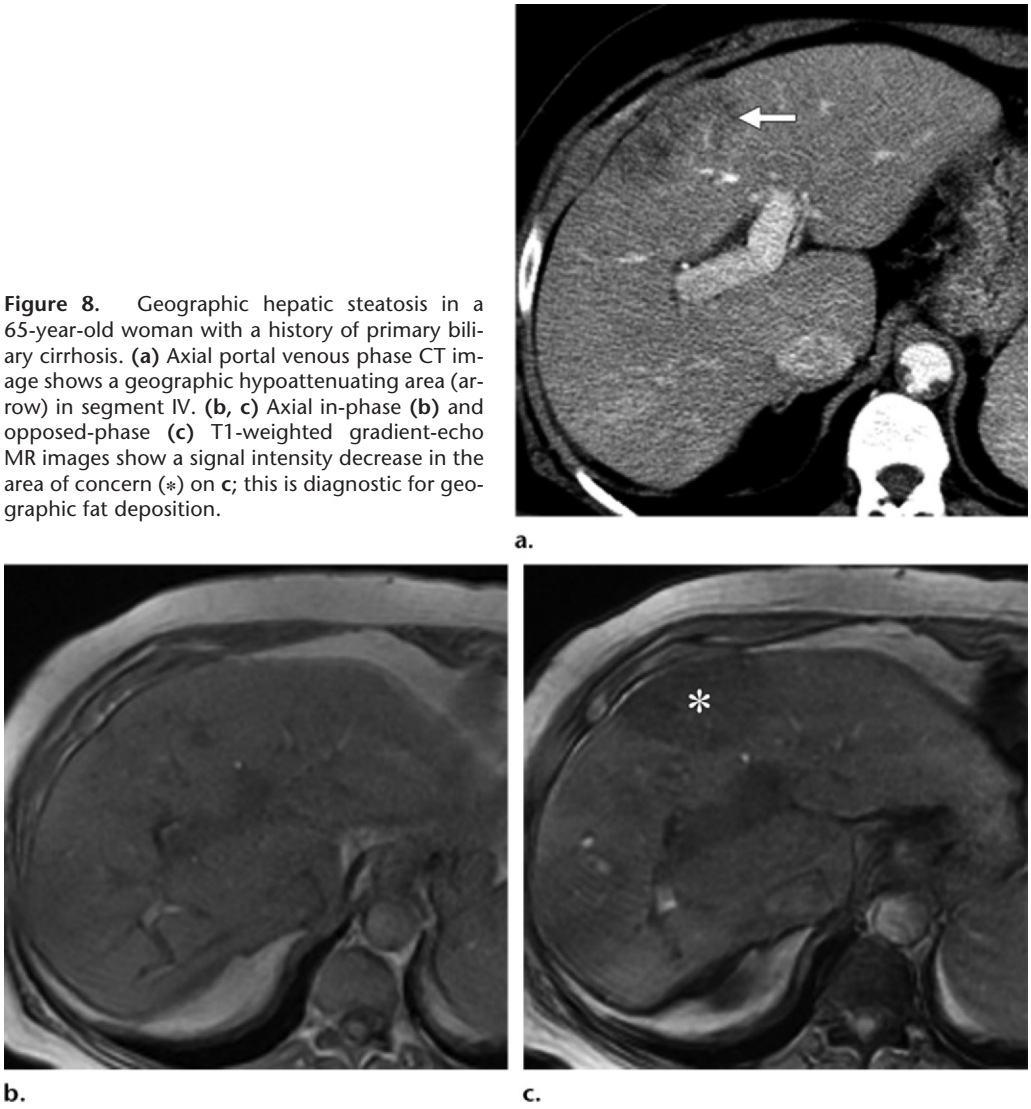

Figure 8. Geographic hepatic steatosis in a 65-year-old woman with a history of primary biliary cirrhosis. **(a)** Axial portal venous phase CT image shows a geographic hypoattenuating area (arrow) in segment IV. **(b, c)** Axial in-phase **(b)** and opposed-phase **(c)** T1-weighted gradient-echo MR images show a signal intensity decrease in the area of concern (∗) on **c**; this is diagnostic for geographic fat deposition.

opposed-phase gradient-echo T1-weighted MR images suggests fat deposition (49) (Fig 8).

Hepatic Microabscesses

Hepatic microabscesses can be an additional cause of multiple hypoattenuating lesions at CT, with associated hyperintensity at T2-weighted MR imaging that results from the presence of necrosis and purulent debris. The cellularity of the latter may produce faint restricted diffusion, a finding that can also be seen in the context of infiltrative HCC. In addition, abscesses may cluster and coalesce, resulting in a heterogeneous pattern of enhancement (Fig 9). Unlike HCC, abscesses typically show peripheral or septal enhancement at contrast-enhanced CT and MR imaging (50). Perilesional hyperintensity on T2-weighted images can also be seen as a result of edema.

Clinical history is often helpful in distinguishing malignancy from an infectious etiology; abscesses may occur in the context of immunosuppression, while in immunocompetent individuals, abscesses can occur in the context of sepsis or a preceding bowel operation. In addition, unlike for HCC, the presence of hepatic infection is independent of the liver morphologic features that do not show a predilection for cirrhosis.

Intrahepatic Cholangiocarcinoma

Cholangiocarcinoma includes a spectrum of different subtypes, with a variety of growth patterns described as exophytic or masslike, periductal or infiltrative, intraductal or polypoid, or a combination of these, depending on the tumor configuration and degree of extension from the biliary system to the adjacent hepatic parenchyma (51,52). Classic masslike intrahepatic cholangiocarcinoma may manifest as an ill-defined mass with a fibrotic pseudocapsule and secondary hepatic capsular retraction. Findings at nonenhanced CT and MR imaging (hypoat-

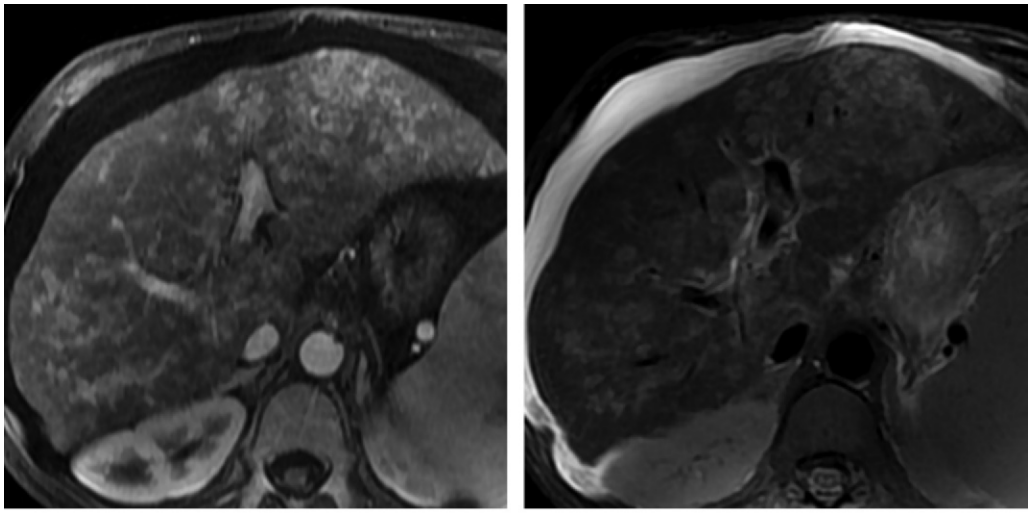

a. b.

Figure 9. Liver microabscesses in a 49-year-old man with a history of hepatitis B virus cirrhosis and colorectal cancer. Axial arterial phase contrast-enhanced T1-weighted **(a)** and axial T2-weighted **(b)** MR images show cirrhotic hepatic morphologic features and innumerable ill-defined nodules that are hyperenhancing on **a** and hyperintense on **b**. The lesions did not show a washout appearance during the delayed phase (not shown). Note the splenomegaly and ascites, compatible with portal hypertension. The portal veins were patent, and the patient's serum AFP level was normal. Examination of a percutaneous fine-needle aspiration biopsy specimen of the lesions showed neutrophilic infiltrates compatible with microabscesses. No micro-organism was isolated.

tenuation and hypointensity on T1-weighted images and hyperintensity on T2-weighted images) are similar to those for HCC. Unlike infiltrative HCC, cholangiocarcinoma may show irregular peripheral enhancement with gradual centripetal enhancement (Fig 10). Components of strong hyperintensity on T2-weighted images may suggest areas of mucin or necrosis, which are atypical for infiltrative HCC (39). Images of the infiltrative subtype of cholangiocarcinoma may show a lobar or segmental periductal growth pattern, resulting in irregular intrahepatic ductal thickening, long-segment duct luminal narrowing, and peripheral duct dilatation, whereas infiltrative HCC may cause intratumoral ductal dilatation (39). Although cholangiocarcinoma typically has better-defined margins, the infiltrative nature of cholangiocarcinoma may make differentiation from infiltrative HCC difficult (39). Finally, although cholangiocarcinoma may compress and displace vessels, it is not typically associated with tumor thrombosis (39,51,52).

Combined hepatocellular and cholangiocellular carcinoma is a rare entity. The tumor is often masslike and contains a variable ratio of hepatocellular and biliary epithelial elements that results in inconsistent heterogeneous imaging features (53,54). Enhancement patterns and ancillary findings are most similar to those of cholangiocarcinoma (54). However, satellite lesions and vascular invasion are confounding findings also seen in infiltrative HCC. Although the combination of imaging features and increase in tumor marker (cancer antigen 19-9 and AFP) levels may suggest the presence of combined hepatocellular and cholangiocellular carcinoma (53,54), examination of tissue samples is often necessary for a final diagnosis.

Diffuse Metastatic Disease (Pseudocirrhosis)

Because infiltrative HCC typically occurs in livers with preexisting cirrhosis, any disease process that distorts the normal hepatic architecture should be regarded as a potential imaging mimic. Pseudocirrhosis related to treated metastatic breast cancer is primary among these, because changes after therapy can include a combination of atrophy, fibrosis, and regeneration, resulting in a dysmorphic configuration and manifestations of portal hypertension—findings similar to those seen in cirrhosis (55–57) (Fig 11). A clinical history of primary cancer (eg, breast cancer) is essential for proper diagnosis.

Treatment and Prognosis for Patients with Infiltrative HCC

The prognosis for patients with infiltrative HCC is poor, with low survival rates, secondary to the advanced stage at presentation and frequent presence of vascular invasion (9,10,40). Survival after surgical resection is decreased; thus, infiltrative HCC is usually a contraindication for resection and transplantation (40,58). The role of intraarterial therapy

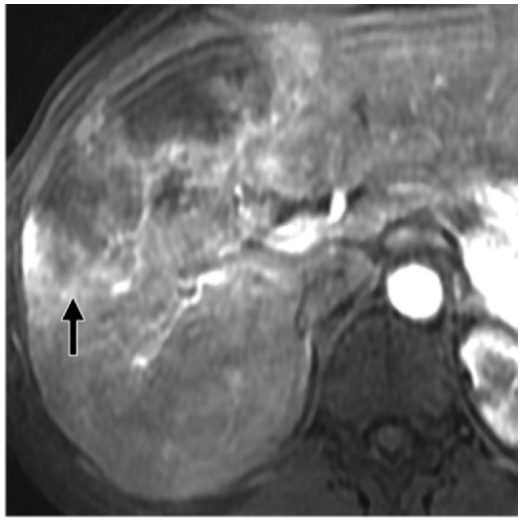

a.

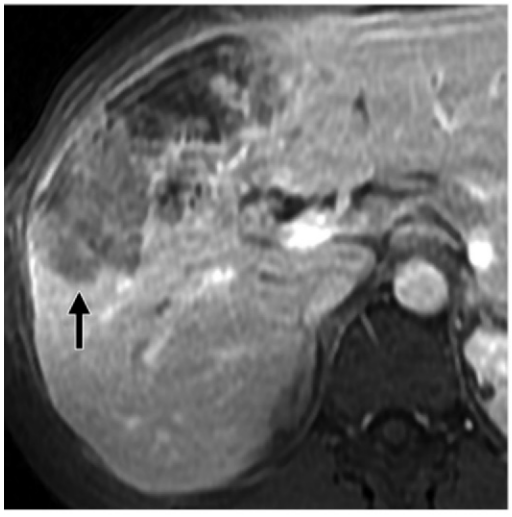

b.

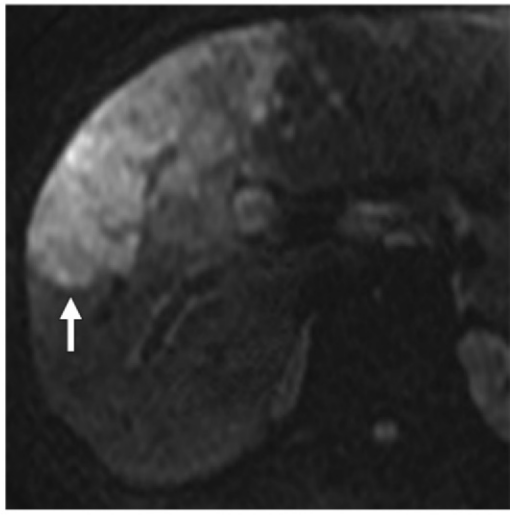

c.

Figure 10. Intrahepatic cholangiocarcinoma in a 43-year-old man with a history of primary sclerosing cholangitis, jaundice, pruritus, and abnormal laboratory values. Both serum carcinoembryonic antigen and cancer antigen 19-9 levels were markedly elevated, and serum AFP level was normal. **(a, b)** Axial contrast-enhanced T1-weighted MR images obtained during the arterial **(a)** and venous **(b)** phases show a large mass (arrow) in segments V and VIII, with irregular peripheral enhancement during the arterial phase and continued centripetal enhancement during the more delayed phases. **(c)** Axial diffusion-weighted image (b = 500 sec/mm^2) shows corresponding high signal intensity (arrow). US-guided biopsy was performed, and the results of examination of the specimen were consistent with poorly to moderately differentiated intrahepatic cholangiocarcinoma. No biliary ductal dilatation or capsular retraction was seen.

a.

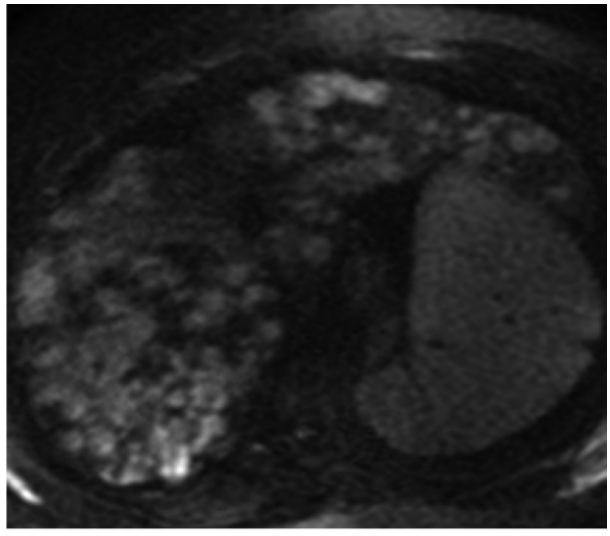

b.

Figure 11. Metastatic breast cancer (pseudocirrhosis) in a 65-year-old woman with a history of metastatic invasive ductal breast carcinoma. **(a)** Axial portal venous phase CT image shows cirrhotic hepatic morphologic features with innumerable nodular lesions throughout both lobes. **(b)** Axial diffusion-weighted image (b = 500 sec/mm^2) shows multiple hyperintense nodules throughout the liver. The portal veins were patent.

such as transarterial chemoembolization in patients with infiltrative HCC is not well defined (40). Lopez et al (59) reported no benefit of transarterial chemoembolization in patients with diffuse HCC, but they did find high postprocedural morbidity and mortality and decreased long-term survival. In a large cohort of patients with infiltrative HCC, however, Kneuertz et al (10) found that intraarterial therapy was well tolerated and beneficial and extended the median survival to 12 months, compared with 3 months when only supportive measures were used. In their series, the majority of patients receiving intraarterial therapy had a Child-Pugh score of A or B, and better results were obtained for patients with a bilirubin level less than 2 mg/dL and an AFP level less than 400 ng/mL at presentation. Similarly, in a recent study, Jang et al (15) suggested that when given to well-selected patients with infiltrative HCC and preserved hepatic function, transarterial chemoembolization is safe and leads to increased survival (>2 years). Overall, systemic chemotherapy is ineffective for patients with HCC (60,61). Recently, sorafenib (a molecular inhibitor of multiple tyrosine kinases) has shown promising results for treatment of advanced HCC (62,63), including the infiltrative subtypes (64,65).

Conclusion

With the increasing incidence of HCC, knowledge of the variable tumor subtypes is critical for appropriate disease diagnosis and treatment. Infiltrative HCC is often difficult to distinguish from underlying cirrhosis, is diagnosed at a late stage, and is associated with a poor prognosis. Knowledge of specific imaging features and the ability to distinguish infiltrative HCC from a variety of diseases with similar findings will allow radiologists to provide critical timely patient care.

References

1. Jemal A, Bray F, Center MM, Ferlay J, Ward E, Forman D. Global cancer statistics. CA Cancer J Clin 2011;61(2):69–90.
2. El-Serag HB. Hepatocellular carcinoma. N Engl J Med 2011; 365(12):1118–1127.
3. El-Serag HB. Epidemiology of viral hepatitis and hepatocellular carcinoma. Gastroenterology 2012;142(6):1264–1273, e1.
4. Altekruse SF, McGlynn KA, Reichman ME. Hepatocellular carcinoma incidence, mortality, and survival trends in the United States from 1975 to 2005. J Clin Oncol 2009;27(9):1485–1491.
5. Forner A, Llovet JM, Bruix J. Hepatocellular carcinoma. Lancet 2012;379(9822):1245–1255.
6. Kojiro M. Histopathology of liver cancers. Best Pract Res Clin Gastroenterol 2005;19(1):39–62.
7. Han YS, Choi DL, Park JB. Cirrhotomimetic type hepatocellular carcinoma diagnosed after liver transplantation: eighteen months of follow-up—a case report. Transplant Proc 2008; 40(8):2835–2836.
8. Jakate S, Yabes A, Giusto D, et al. Diffuse cirrhosis-like hepatocellular carcinoma: a clinically and radiographically undetected variant mimicking cirrhosis. Am J Surg Pathol 2010;34(7):935–941.
9. Benvegnù L, Noventa F, Bernardinello E, Pontisso P, Gatta A, Alberti A. Evidence for an association between the aetiology of cirrhosis and pattern of hepatocellular carcinoma development. Gut 2001;48(1):110–115.
10. Kneuertz PJ, Demirjian A, Firoozmand A, et al. Diffuse infiltrative hepatocellular carcinoma: assessment of presentation, treatment, and outcomes. Ann Surg Oncol 2012;19 (9):2897–2907.
11. Trevisani F, Caraceni P, Bernardi M, et al. Gross pathologic types of hepatocellular carcinoma in Italian patients: relationship with demographic, environmental, and clinical factors. Cancer 1993;72(5):1557–1563.
12. Farinati F, Marino D, De Giorgio M, et al. Diagnostic and prognostic role of alpha-fetoprotein in hepatocellular carcinoma: both or neither? Am J Gastroenterol 2006;101(3):524–532.
13. Kanematsu M, Semelka RC, Leonardou P, Mastropasqua M, Lee JK. Hepatocellular carcinoma of diffuse type: MR imaging findings and clinical manifestations. J Magn Reson Imaging 2003;18(2):189–195.
14. Yuki K, Hirohashi S, Sakamoto M, Kanai T, Shimosato Y. Growth and spread of hepatocellular carcinoma: a review of 240 consecutive autopsy cases. Cancer 1990;66(10): 2174–2179.
15. Jang ES, Yoon JH, Chung JW, et al. Survival of infiltrative hepatocellular carcinoma patients with preserved hepatic function after treatment with transarterial chemoembolization. J Cancer Res Clin Oncol 2013;139(4):635–643.
16. Myung SJ, Yoon JH, Kim KM, et al. Diffuse infiltrative hepatocellular carcinomas in a hepatitis B-endemic area: diagnostic and therapeutic impediments. Hepatogastroenterology 2006;53(68):266–270.
17. Halıloğlu N, Özkavukcu E, Erden A, Erden İ. MR imaging in diffuse-type hepatocellular carcinoma with synchronous portal vein thrombi. Turk J Gastroenterol 2011;22(2): 158–164.
18. European Association for the Study of the Liver; European Organisation for Research and Treatment of Cancer. EASL-EORTC clinical practice guidelines: management of hepatocellular carcinoma. J Hepatol 2012;56(4):908–943.
19. Bruix J, Sherman M; American Association for the Study of Liver Diseases. Management of hepatocellular carcinoma: an update. Hepatology 2011;53(3):1020–1022.
20. HRSA/OPTN data reports. http://optn.transplant.hrsa.gov/PoliciesandBylaws2/policies/pdfs/Policy_8.pdfOPTN. Published October 31, 2013. Accessed March 1, 2014.
21. American College of Radiology. Liver imaging reporting and data system version 2013.1. http://www.acr.org/Quality-Safety/Resources/LIRADS/. Accessed March 1, 2014.
22. Yu NC, Chaudhari V, Raman SS, et al. CT and MRI improve detection of hepatocellular carcinoma, compared with ultrasound alone, in patients with cirrhosis. Clin Gastroenterol Hepatol 2011;9(2):161–167.
23. Colli A, Fraquelli M, Casazza G, et al. Accuracy of ultrasonography, spiral CT, magnetic resonance, and alpha-fetoprotein in diagnosing hepatocellular carcinoma: a systematic review. Am J Gastroenterol 2006;101(3):513–523.
24. Baron RL, Brancatelli G. Computed tomographic imaging of hepatocellular carcinoma. Gastroenterology 2004;127(5,suppl 1):S133–S143.
25. Willatt JM, Hussain HK, Adusumilli S, Marrero JA. MR imaging of hepatocellular carcinoma in the cirrhotic liver: challenges and controversies. Radiology 2008;247(2): 311–330.
26. Wald C, Russo MW, Heimbach JK, Hussain HK, Pomfret EA, Bruix J. New OPTN/UNOS policy for liver transplant allocation: standardization of liver imaging, diagnosis, classification, and reporting of hepatocellular carcinoma. Radiology 2013;266(2):376–382.
27. Bashir MR, Gupta RT, Davenport MS, et al. Hepatocellular carcinoma in a North American population: does hepatobiliary MR imaging with Gd-EOB-DTPA improve sensitivity and confidence for diagnosis? J Magn Reson Imaging 2013; 37(2):398–406.
28. Park MJ, Kim YK, Lee MW, et al. Small hepatocellular carcinomas: improved sensitivity by combining gadoxetic acid–enhanced and diffusion-weighted MR imaging patterns. Radiology 2012;264(3):761–770.

29. Parikh T, Drew SJ, Lee VS, et al. Focal liver lesion detection and characterization with diffusion-weighted MR imaging: comparison with standard breath-hold T2-weighted imaging. Radiology 2008;246(3):812–822.
30. Taouli B, Koh DM. Diffusion-weighted MR imaging of the liver. Radiology 2010;254(1):47–66.
31. Okuda K, Noguchi T, Kubo Y, Shimokawa Y, Kojiro M, Nakashima T. A clinical and pathological study of diffuse type hepatocellular carcinoma. Liver 1981;1(4):280–289.
32. Park YS, Lee CH, Kim BH, et al. Using Gd-EOB-DTPA-enhanced 3-T MRI for the differentiation of infiltrative hepatocellular carcinoma and focal confluent fibrosis in liver cirrhosis. Magn Reson Imaging 2013;31(7):1137–1142.
33. Lim S, Kim YK, Park HJ, Lee WJ, Choi D, Park MJ. Infiltrative hepatocellular carcinoma on gadoxetic acid-enhanced and diffusion-weighted MRI at 3.0T. J Magn Reson Imaging 2014;39(5):1238–1245.
34. Rosenkrantz AB, Lee L, Matza BW, Kim S. Infiltrative hepatocellular carcinoma: comparison of MRI sequences for lesion conspicuity. Clin Radiol 2012;67(12):e105–e111.
35. Dodd GD 3rd, Memel DS, Baron RL, Eichner L, Santiguida LA. Portal vein thrombosis in patients with cirrhosis: does sonographic detection of intrathrombus flow allow differentiation of benign and malignant thrombus? AJR Am J Roentgenol 1995;165(3):573–577.
36. Raza JA, Jang HJ, Kim TK. Differentiating malignant from benign thrombosis in hepatocellular carcinoma: contrast-enhanced ultrasound. Abdom Imaging 2014;39(1):153–161.
37. Dodd GD 3rd, Carr BI. Percutaneous biopsy of portal vein thrombus: a new staging technique for hepatocellular carcinoma. AJR Am J Roentgenol 1993;161(2):229–233.
38. Cedrone A, Rapaccini GL, Pompili M, et al. Portal vein thrombosis complicating hepatocellular carcinoma: value of ultrasound-guided fine-needle biopsy of the thrombus in the therapeutic management. Liver 1996;16(2):94–98.
39. Kim YK, Han YM, Kim CS. Comparison of diffuse hepatocellular carcinoma and intrahepatic cholangiocarcinoma using sequentially acquired gadolinium-enhanced and Resovist-enhanced MRI. Eur J Radiol 2009;70(1):94–100.
40. Demirjian A, Peng P, Geschwind JF, et al. Infiltrating hepatocellular carcinoma: seeing the tree through the forest. J Gastrointest Surg 2011;15(11):2089–2097.
41. Tublin ME, Dodd GD 3rd, Baron RL. Benign and malignant portal vein thrombosis: differentiation by CT characteristics. AJR Am J Roentgenol 1997;168(3):719–723.
42. Shah ZK, McKernan MG, Hahn PF, Sahani DV. Enhancing and expansile portal vein thrombosis: value in the diagnosis of hepatocellular carcinoma in patients with multiple hepatic lesions. AJR Am J Roentgenol 2007;188(5):1320–1323.
43. Catalano OA, Choy G, Zhu A, Hahn PF, Sahani DV. Differentiation of malignant thrombus from bland thrombus of the portal vein in patients with hepatocellular carcinoma: application of diffusion-weighted MR imaging. Radiology 2010;254(1):154–162.
44. Ohtomo K, Baron RL, Dodd GD 3rd, et al. Confluent hepatic fibrosis in advanced cirrhosis: appearance at CT. Radiology 1993;188(1):31–35.
45. Ohtomo K, Baron RL, Dodd GD 3rd, Federle MP, Ohtomo Y, Confer SR. Confluent hepatic fibrosis in advanced cirrhosis: evaluation with MR imaging. Radiology 1993;189(3):871–874.
46. Brancatelli G, Baron RL, Federle MP, Sparacia G, Pealer K. Focal confluent fibrosis in cirrhotic liver: natural history studied with serial CT. AJR Am J Roentgenol 2009;192(5):1341–1347.
47. Marin D, Iannaccone R, Catalano C, Passariello R. Multinodular focal fatty infiltration of the liver: atypical imaging findings on delayed T1-weighted Gd-BOPTA-enhanced liver-specific MR images. J Magn Reson Imaging 2006;24(3):690–694.
48. Yeom SK, Byun JH, Kim HJ, et al. Focal fat deposition at liver MRI with gadobenate dimeglumine and gadoxetic acid: quantitative and qualitative analysis. Magn Reson Imaging 2013;31(6):911–917.
49. Pokharel SS, Macura KJ, Kamel IR, Zaheer A. Current MR imaging lipid detection techniques for diagnosis of lesions in the abdomen and pelvis. RadioGraphics 2013;33(3):681–702.
50. Mortelé KJ, Segatto E, Ros PR. The infected liver: radiologic-pathologic correlation. RadioGraphics 2004;24(4):937–955.
51. Lee WJ, Lim HK, Jang KM, et al. Radiologic spectrum of cholangiocarcinoma: emphasis on unusual manifestations and differential diagnoses. RadioGraphics 2001;21(Spec No):S97–S116.
52. Chung YE, Kim MJ, Park YN, et al. Varying appearances of cholangiocarcinoma: radiologic-pathologic correlation. RadioGraphics 2009;29(3):683–700.
53. de Campos RO, Semelka RC, Azevedo RM, et al. Combined hepatocellular carcinoma-cholangiocarcinoma: report of MR appearance in eleven patients. J Magn Reson Imaging 2012;36(5):1139–1147.
54. Fowler KJ, Sheybani A, Parker RA 3rd, et al. Combined hepatocellular and cholangiocarcinoma (biphenotypic) tumors: imaging features and diagnostic accuracy of contrast-enhanced CT and MRI. AJR Am J Roentgenol 2013;201(2):332–339.
55. Jha P, Poder L, Wang ZJ, Westphalen AC, Yeh BM, Coakley FV. Radiologic mimics of cirrhosis. AJR Am J Roentgenol 2010;194(4):993–999.
56. Young ST, Paulson EK, Washington K, Gulliver DJ, Vredenburgh JJ, Baker ME. CT of the liver in patients with metastatic breast carcinoma treated by chemotherapy: findings simulating cirrhosis. AJR Am J Roentgenol 1994;163(6):1385–1388.
57. Jüngst C, Krämer J, Schneider G, Lammert F, Zimmer V. Subacute liver failure by pseudocirrhotic metastatic breast cancer infiltration. Ann Hepatol 2013;12(5):834–836.
58. Ochiai T, Sonoyama T, Ichikawa D, et al. Poor prognostic factors of hepatectomy in patients with resectable small hepatocellular carcinoma and cirrhosis. J Cancer Res Clin Oncol 2004;130(4):197–202.
59. Lopez RR Jr, Pan SH, Hoffman AL, et al. Comparison of transarterial chemoembolization in patients with unresectable, diffuse vs focal hepatocellular carcinoma. Arch Surg 2002;137(6):653–657; discussion 657–658.
60. Lin S, Hoffmann K, Schemmer P. Treatment of hepatocellular carcinoma: a systematic review. Liver Cancer 2012;1(3-4):144–158.
61. Thomas MB, O'Beirne JP, Furuse J, Chan AT, Abou-Alfa G, Johnson P. Systemic therapy for hepatocellular carcinoma: cytotoxic chemotherapy, targeted therapy and immunotherapy. Ann Surg Oncol 2008;15(4):1008–1014.
62. Llovet JM, Ricci S, Mazzaferro V, et al. Sorafenib in advanced hepatocellular carcinoma. N Engl J Med 2008;359(4):378–390.
63. Bruix J, Raoul JL, Sherman M, et al. Efficacy and safety of sorafenib in patients with advanced hepatocellular carcinoma: subanalyses of a phase III trial. J Hepatol 2012;57(4):821–829.
64. Kim HY, Park JW, Nam BH, et al. Survival of patients with advanced hepatocellular carcinoma: sorafenib versus other treatments. J Gastroenterol Hepatol 2011;26(11):1612–1618.
65. Mehta N, Fidelman N, Sarkar M, Yao FY. Factors associated with outcomes and response to therapy in patients with infiltrative hepatocellular carcinoma. Clin Gastroenterol Hepatol 2013;11(5):572–578.